SLAC–PUB–8318
December 1999

Lecture on Beam Instabilities*

Alex Chao
Stanford Linear Accelerator Center, Stanford Unversity, CA 94309

Abstract

These lectures treat some of the common collective beam instability effects encountered in accelerators. In choosing the material for these lectures, it is attempted to introduce this subject with a more practical approach, instead of a more theoretical approach starting with first principles. After introducing the terminologies, emphasis will be placed on how to apply the lecture material to perform calculations and to make estimates of various instability effects.

In the first half of the lectures, after briefly introducing the concepts of impedance and wake field, we will discuss a selected list of formulas for the impedances of various accelerator components. Detailed derivations are omitted, allowing time for the students to think through the process of how to apply the knowledge learned. The list of impedances to be covered include: space charge, resistive wall, resonator, wall roughness, and small perturbation on the vacuum chamber wall.

Assuming impedances are known, the second half of the lectures addresses the question of how to calculate the power of beam heating, the growth rates, and the thresholds for a list of selected beam instability effects. Again with minimal detailed derivations, our aim is to introduce a collection of formulas, and apply them to linear as well as circular accelerators. The list of beam instability effects to be covered include: loss factor, beam break-up, BNS damping, bunch lengthening, resistive wall instability, head-tail instability, longitudinal head-tail instability, Landau damping, microwave instability, and mode coupling instability.

Lectures at the Asian School on Electron Storage Rings
Huairou, China
November 22 - December 4, 1999

*Work supported by Department of Energy contract DE–AC03–76SF00515.

1 Wakefields

When a charged particle beam traverses a discontinuity in the conducting vacuum chamber, an electromagnetic *wakefield* is generated, as sketched in Fig.1. An intense beam will generate a strong wakefield. When the wakefield is strong enough, the beam becomes unstable.

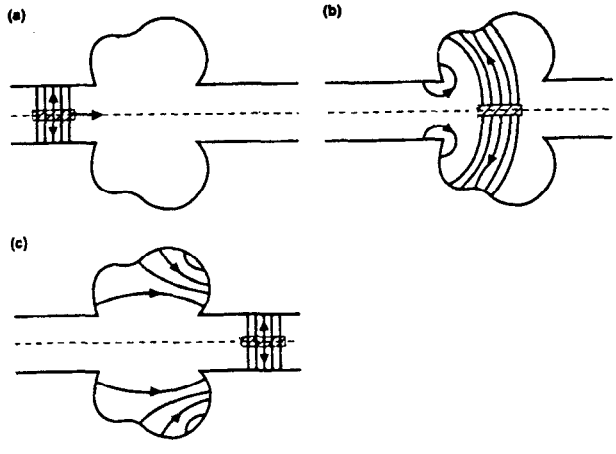

Figure 1: Wakefield driven by a beam when there is a discontinuity in the vacuum chamber. (a) before the drive beam traverses the vacuum chamber discontinuity, (b) during the traversal, (c) after the traversal.

Let the drive beam have charge q and travels down the beam pipe along its axis. Consider a test charge e following the drive beam. Let both the drive beam and the test charge move with speed $v \approx c$, holding the spacing z between them fixed. Let $\vec{E}$ and $\vec{B}$ be the electric and magnetic parts of the wakefield seen by the test charge. The test charge experiences the wake force $\vec{F} = e(\vec{E} + \vec{v} \times \vec{B})$.

Integrating $\vec{F}$ over the traversal results in the *wake potential*

$$\overline{\vec{F}} = \int_{-\infty}^{\infty} ds \vec{F} \tag{1}$$

$\overline{\vec{F}}$ is a function of the spacing between the test charge and the drive beam z. It also depends on (r, θ), the transverse coordinates of the test charge. Furthermore, it satisfies the *Panofsky-Wenzel theorem*,

$$\nabla_\perp \overline{F}_\parallel = \frac{\partial}{\partial z} \overline{\vec{F}}_\perp \tag{2}$$

Here $\parallel$ denotes longitudinal and $\perp$ denotes transverse components.

One can also consider a drive beam which travels down the axis of the beam pipe with an mth moment I_m. ($m = 0, 1, 2$ correspond to monopole, dipole and quadrupole moments. When $m = 0$, one has $I_0 = q$.) In case the discontinuity is axially symmetric, one can write

$$\begin{aligned} \overline{\vec{F}}_\perp(r, \theta, z) &= -eI_m W_m(z)\, m r^{m-1} (\hat{r} \cos m\theta - \hat{\theta} \sin m\theta) \\ \overline{F}_\parallel(r, \theta, z) &= -eI_m W'_m(z)\, r^m \cos m\theta \end{aligned} \tag{3}$$

Here a prime denotes d/dz. $W_m(z)$ is called the *transverse wake function* and $W'_m(z)$ the *longitudinal wake function.*

We omit its derivation, but Eq.(3) is quite amazing. An efficient application of the Maxwell equations has yielded a wealth of information built-in in Eq.(3). The fact that $\overline{\vec{F}}$ is proportional to e and I_m is straightforward. On the other hand, without even specifying the geometry of the vacuum chamber discontinuity, or the chamber wall's resistivity, one sees that the m, r, and θ dependences of the wake potentials have been explicitly solved. The only unknown

in Eq.(3) is the wake function $W_m(z)$, which depends only on z. Furthermore, the transverse and the longitudinal wake potentials involve the *same* funtion $W_m(z)$.

Homework

One consequence of the Maxwell equations is the Panofsky-Wenzel theorem. Show that the Panofsky-Wenzel theorem is built-in in Eq.(3).

In Cartesian coordinates, for each of the mth moment, the drive beam has two components—one normal and another skewed. Table below lists the two moments (first the normal moment and then the skewed moment) and the associated transverse and longitudinal wake potentials seen by a test charge e with transverse coordinates x, y that follows, at a distance $|z|$ behind, a beam which possesses an mth moment. The question being asked is what kick is being received by the test charge e as the beam and the test charge complete the traversal of the chamber discontinuity. We have the convention that $z < 0$ if the test charge trails the drive beam. A bracket $\langle\ \rangle$ means averaging over the transverse distribution of the drive beam; $\hat{x}$ and $\hat{y}$ are the unit vectors in the x-

and y-directions.

m	Distribution Moments of Beam	Longitudinal Wake Potential	Transverse Wake Potential
0	q	$-eq\,W_0'(z)$	0
1	$q\langle x\rangle$	$-eq\langle x\rangle x W_1'(z)$	$-eq\langle x\rangle W_1(z)\hat{x}$
	$q\langle y\rangle$	$-eq\langle y\rangle y W_1'(z)$	$-eq\langle y\rangle W_1(z)\hat{y}$
2	$q\langle x^2-y^2\rangle$	$-eq\langle x^2-y^2\rangle(x^2-y^2)W_2'(z)$	$-2eq\langle x^2-y^2\rangle W_2(z)(x\hat{x}-y\hat{y})$
	$q\langle 2xy\rangle$	$-eq\langle 2xy\rangle 2xy\,W_2'(z)$	$-2eq\langle 2xy\rangle W_2(z)(y\hat{x}+x\hat{y})$
3	$q\langle x^3-3xy^2\rangle$	$-eq\langle x^3-3xy^2\rangle \times(x^3-3xy^2)W_3'(z)$	$-3eq\langle x^3-3xy^2\rangle W_3(z) \times[(x^2-y^2)\hat{x}-2xy\hat{y}]$
	$q\langle 3x^2y-y^3\rangle$	$-eq\langle 3x^2y-y^3\rangle \times(3x^2y-y^3)W_3'(z)$	$-3eq\langle 3x^2y-y^3\rangle W_3(z) \times[2xy\hat{x}+(x^2-y^2)\hat{y}]$

(4)

Eq.(4) contains rich information about the wake effects and should be studied with attention. Note that the leading longitudinal wake potential is driven by the monopole ($m = 0$) moment of the drive beam, while the leading transverse wake potential is driven by the dipole moment ($m = 1$) of the beam. However, when the geometry is not axially symmetric, one must not forget that a monopole beam moment can also drive transverse wake potential.

Dimensionalities of the wake functions are $[W_m] = [\Omega \mathrm{s}^{-1}\mathrm{m}^{-2m+1}]$, $[W_m'] = [\Omega \mathrm{s}^{-1}\mathrm{m}^{-2m}]$. The most important transverse wake function is that for $m = 1$, $[W_1] = [\Omega \mathrm{s}^{-1}\mathrm{m}^{-1}]$. The most important longitudinal wake function has $m = 0$, $[W_0'] = [\Omega \mathrm{s}^{-1}]$.

Properties of wake functions

- $W_m(z) = 0$, $W'_m(z) = 0$ for $z > 0$ (causality).
- $W_m(z) \leq 0$, $W'_m(z) \geq 0$ for $z \rightarrow 0^-$.
- $W_m(0) = 0$ (in most cases, except space charge).
- $W'_m(0) = \frac{1}{2} W'_m(0^-)$ (fundamental theorem of beam loading).
- $W'_m(0^-) \geq |W'_m(z)|$ for all z.
- $\int_{-\infty}^{0} W'_m(z) dz \geq 0$.

In general, $W_m(z)$ is a sine-like function, while $W'_m(z)$ is a cosine-like function, as sketched below.

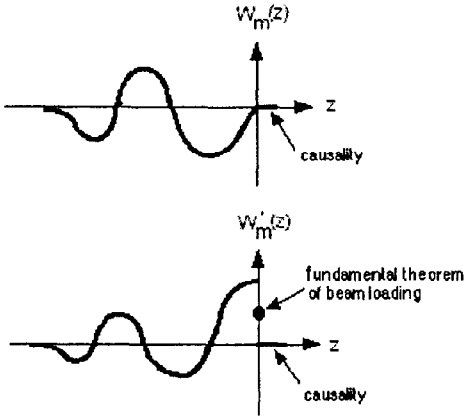

2 Impedances

Impedances are just Fourier transforms of wake functions:

$$\begin{aligned} Z_m^{\parallel}(\omega) &= \int_{-\infty}^{\infty} \frac{dz}{v} e^{-i\omega z/v} W'_m(z) \\ Z_m^{\perp}(\omega) &= \frac{i}{v/c} \int \frac{dz}{v} e^{-i\omega z/v} W_m(z) \end{aligned} \tag{5}$$

Time dependence of $e^{-i\omega t}$ is assumed.

Dimensionalities are $[Z_m^{\parallel}] = [\Omega \mathrm{m}^{-2m}], [Z_m^{\perp}] = [\Omega \mathrm{m}^{-2m+1}]$. The most important transverse impedance is that for $m = 1$, $[Z_1^{\perp}] = [\Omega \mathrm{m}^{-1}]$. The most important longitudinal impedance has $m = 0$, $[Z_0^{\parallel}] = [\Omega]$.

Properties of impedances

- $Z_m^{\parallel}(\omega) = \dfrac{\omega}{c} Z_m^{\perp}(\omega)$ (Panofsky-Wenzel theorem in frequency domain).
- $\begin{cases} Z_m^{\parallel\,*}(\omega) = Z_m^{\parallel}(-\omega) \\ Z_m^{\perp\,*}(\omega) = -Z_m^{\perp}(-\omega) \end{cases}$ (reality of wake functions).
- $\begin{cases} \int_0^{\infty} d\omega \, \mathrm{Im} Z_m^{\perp}(\omega) = 0 \\ \int_0^{\infty} d\omega \, \dfrac{\mathrm{Im} Z_m^{\parallel}(\omega)}{\omega} = 0 \\ \mathrm{Re} Z_m^{\parallel}(0) = 0 \end{cases}$ ($W_m(0) = 0$, in most cases).
- $\begin{cases} \mathrm{Re} Z_m^{\parallel}(\omega) = \dfrac{1}{\pi} \mathrm{PV} \displaystyle\int_{-\infty}^{\infty} d\omega' \, \frac{\mathrm{Im} Z_m^{\parallel}(\omega')}{\omega' - \omega} \\ \mathrm{Im} Z_m^{\parallel}(\omega) = -\dfrac{1}{\pi} \mathrm{PV} \displaystyle\int_{-\infty}^{\infty} d\omega' \, \frac{\mathrm{Re} Z_m^{\parallel}(\omega')}{\omega' - \omega} \end{cases}$
(causality, Hilbert transform)

The same expressions apply to $Z_m^{\perp}$. PV means taking the principal value of the integral.

- $\begin{cases} \mathrm{Re} Z_m^{\parallel}(\omega) \geq 0 \text{ for all } \omega \\ \mathrm{Re} Z_m^{\perp}(\omega) \geq 0 \text{ if } \omega > 0, \quad \leq 0 \text{ if } \omega < 0 \end{cases}$
- $Z_1^{\perp} \approx \dfrac{2c}{b^2 \omega} Z_0^{\parallel}$, $Z_m^{\perp} \approx \dfrac{2c}{b^{2m} \omega} Z_0^{\parallel}$, $Z_m^{\parallel} \approx \dfrac{2}{b^{2m}} Z_0^{\parallel}$

These are approximate expressions relating transverse and longitudinal impedances, $b =$ pipe radius. They are exact for resistive round pipe.

3 Calculation of Impedances

To calculate the impedance for a given vacuum chamber discontinuity, one needs to solve for the electromagnetic fields produced in the vacuum chamber by a given beam current. Over the years, a large arsenal of techniques have been developed to calculate the impedances.

The first method is to solve Maxwell equations analytically with appropriate boundary conditions. This method applies only to the simplest cases. We omit the derivations and give only the results for some examples.

Space charge See Fig.2 for the wakefield patterns in the transverse plane. The z-dependence is a δ-function $\delta(z)$. With a beam of radius a in a perfectly conducting round pipe of radius b and length L,

Impedances	Wake functions
$Z_0^{\parallel} = i\dfrac{Z_0 L\omega}{4\pi c\gamma^2}\left(1+2\ln\dfrac{b}{a}\right)$	$W_0' = \dfrac{Z_0 cL}{4\pi\gamma^2}\left(1+2\ln\dfrac{b}{a}\right)\delta'(z)$
$Z_{m\neq 0}^{\perp} = i\dfrac{Z_0 L}{2\pi\gamma^2 m}\left(\dfrac{1}{a^{2m}}-\dfrac{1}{b^{2m}}\right)$	$W_{m\neq 0} = \dfrac{Z_0 cL}{2\pi\gamma^2 m}\left(\dfrac{1}{a^{2m}}-\dfrac{1}{b^{2m}}\right)\delta(z)$

(6)

where $Z_0 = \sqrt{\mu_0/\epsilon_0} \approx 377\ \Omega$ is the free-space impedance, ϵ_0 and μ_0 are the free-space dielectric constant and magnetic permeability. Because of the factor $1/\gamma^2$, space charge effects are most significant for low-to-medium energy proton or heavy ion accelerators.

The space charge impedance is purely imaginary, and is proportional to $i\omega$. Its ω-dependence is as if it is a pure inductance. However, its sign is as if it is a capacitance. By convention, we call the space charge impedance "capacitive".

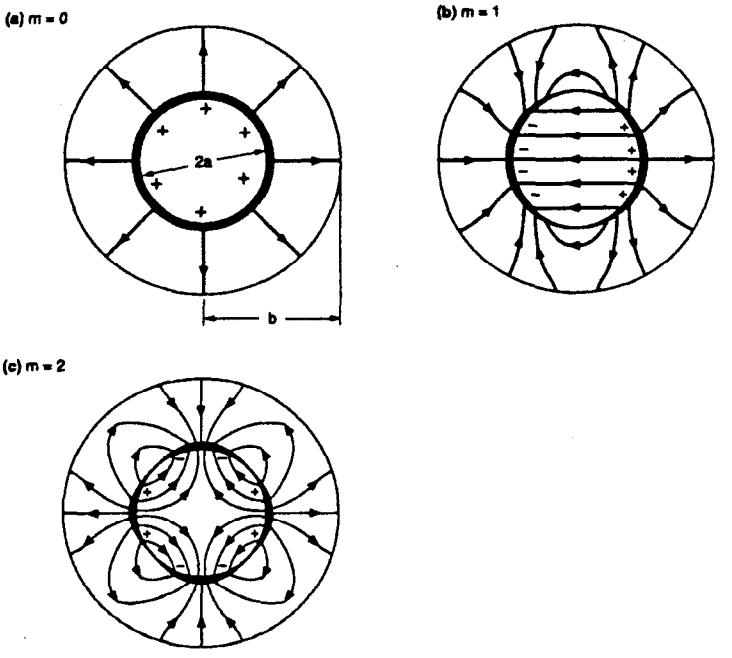

Figure 2: Space charge wakefields in the x-y plane which contains the ring-shaped, infinitely thin, $\cos m\theta$-distribution drive beam.

Resistive wall Another case solvable analytically is for a round resistive pipe with radius b, conductivity σ_c, and length L. Defining the skin depth (change 0.066 to 0.086 for aluminum, and to 0.43 for stainless steel)

$$\delta_{\rm skin} = \sqrt{\frac{2c}{|\omega| Z_0 \sigma_c}}, \qquad \delta_{\rm skin}\,[\rm mm] = \frac{0.066}{\sqrt{f\,[\rm MHz]}} \text{ for copper, room temp.} \quad (7)$$

one finds

Impedances	Wake functions
$Z_m^{\parallel} = \dfrac{\omega}{c} Z_m^{\perp}$	$W_m = -\dfrac{c}{\pi b^{m+1}(1+\delta_{m0})} \sqrt{\dfrac{Z_0}{\pi\sigma_c}} \dfrac{L}{\lvert z\rvert^{1/2}}$
$Z_m^{\parallel} = \dfrac{1-\mathrm{sgn}(\omega) i}{1+\delta_{0m}} \dfrac{L}{\pi\sigma_c \delta_{\rm skin} b^{2m+1}}$	$W_m' = -\dfrac{c}{2\pi b^{m+1}(1+\delta_{m0})} \sqrt{\dfrac{Z_0}{\pi\sigma_c}} \dfrac{L}{\lvert z\rvert^{3/2}}$

(8)

The impedance is proportional to $(1-i)$, i.e. one might say that it is half resistive and half inductive.

Displaced beam in a resistive pipe If the beam is not centered, but is displaced a distance x_0 in the beam pipe, the impedances can still be found analytically,

$$\begin{aligned} Z_0^{\parallel} &= \frac{[1-\mathrm{sgn}(\omega)i]L}{2\pi\sigma_c\delta_{\mathrm{skin}}b} \times \frac{b^2+x_0^2}{b^2-x_0^2} \\ Z_1^{\{x,y\}} &= \frac{[1-\mathrm{sgn}(\omega)i]cL}{\pi\omega\sigma_c\delta_{\mathrm{skin}}b} \times \frac{b^4}{(b^2-x_0^2)^3}\{b^2+3x_0^2, b^2-x_0^2\} \end{aligned} \tag{9}$$

Eq.(9) is useful when the beam is close to the chamber wall, such as in the case of a metallic collimator. On the other hand, in those cases, one should also include contribution from the wall surface roughness (see later).

Field matching method For more complicated cases, solutions are often to be found numerically. For example, in structures which can be subdivided into a few simple subregions (e.g., Fig.3 for the case of a pill-box cavity), a field matching method can be applied. Solution in each subregion is expanded in terms of the eigen functions of the respective subregion with yet-to-be-determined coefficients. Field matching on the subregion interfaces and boundary conditions on the vacuum chamber walls leads to an infinite system of linear equations for these coefficients, which usually can be truncated to a finite size.

Pill-box cavity The pill-box cavity is a complicated object. Its accurate impedances are to be found numerically. However, approximate impedances of a pill-box cavity can be found by combining the following:

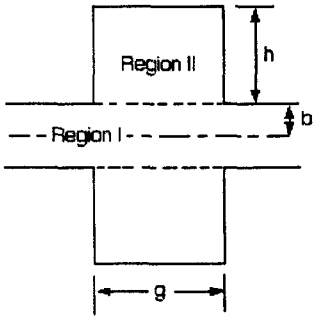

Figure 3: Pill-box cavity and field matching method.

(i) Resonant impedances: A pill-box cavity can trap some modes, each giving rise to a sharp, narrow-band impedance. The resonant frequencies are determined approximately ($d = h + b$) by (ignoring pipe radius b, up to frequency $\omega \sim c/b$)

$$\frac{\omega_{mnp}^2}{c^2} = \frac{x_{mn}^2}{d^2} + \frac{p^2\pi^2}{g^2} \tag{10}$$

where n, p, m are the radial, longitudinal, and azimuthal mode indices, x_{mn} is the nth zero of Bessel function J_m. The shunt impedance R_s and the Q-value of the modes satisy

$$\left[\frac{R_s}{Q}\right]_{0np} = \frac{Z_0}{x_{0n}^2 J_0'^2(x_{0n})} \frac{8c}{\pi g \omega_{0np}} \begin{cases} \sin^2 \frac{g\omega_{0np}}{2\beta c} \times (1+\delta_{0p}) & p \text{ even} \\ \cos^2 \frac{g\omega_{0np}}{2\beta c} & p \text{ odd} \end{cases}$$

$$\left[\frac{R_s}{Q}\right]_{1np} = \frac{Z_0}{J_1'^2(x_{1n})} \frac{2c^2}{\pi g d^2 \omega_{1np}^2} \begin{cases} \sin^2 \frac{g\omega_{1np}}{2\beta c} \times (1+\delta_{0p}) & p \text{ even} \\ \cos^2 \frac{g\omega_{1np}}{2\beta c} & p \text{ odd} \end{cases} \tag{11}$$

(ii) Low-frequency broad-band impedance: In addition to trapped modes, a pill-box cavity also gives rise to a broad-band impedance. At low frequencies $\omega \ll c/b$, and for a small pill-box ($g, h \ll b$) this part of impedance behaves as

an inductance,

Impedances	Wake functions
$Z_0^{\parallel}=\begin{cases}-i\frac{\omega Z_0}{2\pi cb}\left(gh-\frac{g^2}{2\pi}\right) & g\le h\\ -i\frac{\omega Z_0 h^2}{\pi^2 cb}\left(\ln\frac{2\pi g}{h}+\frac{1}{2}\right) & h\ll g\end{cases}$	$W_0'=\begin{cases}-\frac{Z_0 c}{2\pi b}\left(gh-\frac{g^2}{2\pi}\right)\delta'(z) & g\le h\\ -\frac{Z_0 ch^2}{\pi^2 b}\left(\ln\frac{2\pi g}{h}+\frac{1}{2}\right)\delta'(z) & h\ll g\end{cases}$
$Z_1^{\perp}=\begin{cases}-i\frac{Z_0}{\pi b^3}\left(gh-\frac{g^2}{2\pi}\right) & g\le h\\ -i\frac{2Z_0 h^2}{\pi^2 b^3}\left(\ln\frac{2\pi g}{h}+\frac{1}{2}\right) & h\ll g\end{cases}$	$W_1=\begin{cases}-\frac{Z_0 c}{\pi b^3}\left(gh-\frac{g^2}{2\pi}\right)\delta(z) & g\le h\\ -\frac{2Z_0 ch^2}{\pi^2 b^3}\left(\ln\frac{2\pi g}{h}+\frac{1}{2}\right)\delta(z) & h\ll g\end{cases}$

(12)

(iii) High-frequency broad-band impedance: Diffraction theory can be used to calculate the impedances at high frequencies, $\omega \gg c/b$, yielding

Impedances	Wake functions
$Z_m^{\parallel}=\frac{[1+\mathrm{sgn}(\omega)i]Z_0}{(1+\delta_{m0})\pi^{3/2}b^{2m+1}}\sqrt{\frac{cg}{\lvert\omega\rvert}}$	$W_m=-\frac{2Z_0c\sqrt{2g}}{(1+\delta_{m0})\pi^2 b^{2m+1}}\lvert z\rvert^{1/2}$
$Z_m^{\parallel}=\frac{\omega}{c}Z_m^{\perp}$	$W_m'=\frac{Z_0c\sqrt{2g}}{(1+\delta_{m0})\pi^2 b^{2m+1}}\lvert z\rvert^{-1/2}$

(13)

The impedance $Z_0^{\parallel} \propto 1+i$, i.e. half resistive and half capacitive.

Broad band resonator model If one is interested only in the short range wake, a cavity whose dimensions are comparable to the pipe radius b can be approximated by a broad band resonator (see Eq.(18) for resonator model in general). The impedances *per cavity* are approximated by

$$\begin{aligned} R_S^{(0)} &\approx 60\Omega, \quad Q\approx 1, \quad \omega_r \approx \frac{c}{b} \quad \text{for } Z_0^{\parallel}\\ R_S^{(1)} &\approx 60\Omega \times \frac{1}{b^2}, \quad Q\approx 1, \quad \omega_r \approx \frac{c}{b} \quad \text{for } Z_1^{\perp} \end{aligned} \tag{14}$$

If one further contends by finding only an order-of-magnitude estimate, one can take the impedance values at $\omega \sim \omega_r$ (or equivalently the wake function values

at $|z| \sim b$), and obtains, very roughly, per cavity,

Impedances	Wake functions
$Z_m^{\parallel} \sim \frac{Z_0}{4\pi}\frac{1}{b^{2m}}$	$W_m \sim \frac{Z_0 c}{4\pi}\frac{1}{b^{2m}}$
$Z_m^{\perp} \sim \frac{Z_0}{4\pi}\frac{1}{b^{2m-1}}$	$W'_m \sim \frac{Z_0 c}{4\pi}\frac{1}{b^{2m+1}}$

(15)

In particular, $Z_0^{\parallel} \sim 30\ \Omega$ and $Z_1^{\perp} \sim 30\,\Omega/b$. Note that $Z_0^{\parallel}$ per cavity is independent of the cavity size or the pipe radius b as long as they are comparable. The longitudinal wake function can be rewritten in another convenient form as W'_0 [V/pC] $\sim 0.9/b$ [cm]. Eq.(15) is useful for linacs with its accelerating cavities of dimensions $\sim b$.

Periodic pill-box array For an array of pill-boxes, each with gap length g, box spacing L, and beam pipe radius b, the high-frequency impedance per box is ($k = \omega/c$)

$$Z_0^{\parallel} = \frac{iZ_0 L}{\pi k b^2}\left[1 + (1 + i\,\mathrm{sgn}(k))\frac{\alpha L}{b}\sqrt{\frac{\pi}{|k|g}}\right]^{-1} \tag{16}$$

$$\alpha = \begin{cases} 1 & \text{when } g/L \ll 1 \\ 0.4648 & \text{when } g/L = 1, \text{infinitely thin irises} \end{cases}$$

The real part of $Z_0^{\parallel}$ goes like $\sim k^{-3/2}$ for large k, while the imaginary part goes like $\sim k^{-1}$. This is in contrast with a single pill-box, whose impedance (both real and imaginary parts, see Eq.(13)) at high frequencies behave like $\sim \omega^{-1/2}$.

In addition to Eq.(16) and the trapped modes, there is a resonator-type impedance generated by the pill-box array. If the boxes are small, they contribute to a single-frequency impedance mode at $k_0 = \omega_0/c = \sqrt{2L/bg\delta}$ (δ is cavity depth),

Impedances	Wake functions
$\frac{Z_0^{\parallel}}{L} = \frac{Z_0 c}{2\pi b^2}\left[\pi\delta(\omega-\omega_0)+\pi\delta(\omega+\omega_0)+\frac{i}{\omega-\omega_0}+\frac{i}{\omega+\omega_0}\right]$	$\frac{W_1(z)}{L} = \frac{2Z_0 c}{\pi b^4 k_0}\sin k_0 z$
$\frac{Z_1^{\perp}}{L} = \frac{2c}{b^2\omega}\frac{Z_0^{\parallel}}{L}$	$\frac{W_0'(z)}{L} = \frac{Z_0 c}{\pi b^2}\cos k_0 z$

(17)

The corresponding resonator has $(\frac{1}{L})(R_s^{(0)}/Q) = Z_0/(\pi b^2 k_0)$.

Time domain calculations Another way to calculate the impedances numerically is to do it in the time domain. By evolving the Maxwell equations on a mesh, wakefields driven by a rigid ultra-short gaussian beam are calculated as functions of time. Integrating the wakefields seen by a test charge that trails the drive beam produces the wake functions. Fourier transforming the wake functions then gives the impedances. Fig.4 is an example of such a calculation using the program MAFIA.

Resonator model Sometimes it is useful to model an impedance by an equivalent circuit. In this approach, a complicated object is modeled as a transmission line or as an *RLC*-circuit. The most notable example is the resonator model ($R_s^{(m)}$ is the shunt impedance, Q is the quality factor, ω_r is the resonant frequency),

Impedances	Wake functions
$Z_m^{\parallel} = \frac{R_s^{(m)}}{1+iQ\,(\omega_r/\omega-\omega/\omega_r)}$	$W_m(z<0) = \frac{R_s^{(m)} c\,\omega_r}{Q\bar{\omega}_r}\,e^{\alpha z/c}\sin\frac{\bar{\omega}_r z}{c}$
$Z_m^{\perp} = \frac{c}{\omega}Z_m^{\parallel}$	$\alpha = \omega_r/(2Q),\ \bar{\omega}_r = \sqrt{\lvert\omega_r^2-\alpha^2\rvert}$

(18)

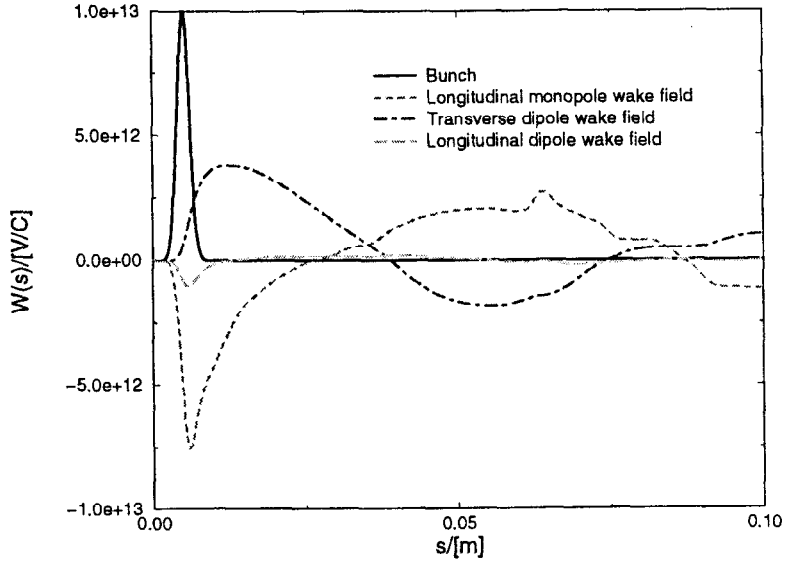

Figure 4: The longitudinal and transverse wake potentials of a 3-cell structure obtained by a time domain calculation. The drive beam has $\sigma_z = 1$mm. The offset of the drive beam and the test charge is 1 mm.

Stripline beam-position monitor Another example of an equivalent circuit impedance is that for strip-line BPMs (two strip lines of length L, subtending angle per strip ϕ_0, forming transmission lines of characteristic impedance Z_c).

Impedances	Wake functions
$Z_0^{\parallel} = 2Z_c\left(\frac{\phi_0}{2\pi}\right)^2\left[2\sin^2\frac{\omega L}{c} - i\sin\frac{2\omega L}{c}\right]$	$W_0' = 2Z_c\, c\left(\frac{\phi_0}{2\pi}\right)^2[\delta(z) - \delta(z+2L)]$
$Z_1^{\perp} = Z_0^{\parallel}\frac{c}{b^2\omega}\left(\frac{4}{\phi_0}\right)^2\sin^2\frac{\phi_0}{2}$	$W_1 = \frac{8Z_c c}{\pi^2 b^2}\sin^2\frac{\phi_0}{2}[H(z) - H(z+2L)]$

(19)

Slowly varying wall boundaries If the vacuum chamber wall varies along the accelerator slowly, a perturbation technique can be used to calculate the impedances. Specify the wall variation by $h(z)$ (1-D axisymmetric bump), or

$h(z,\theta)$ (2-D bump). At low frequencies $k = \omega/c \ll$ (bump length or width)$^{-1}$, $|h| \ll b$, and $|\nabla h| \ll 1$, the impedance is purely inductive,

$$\underline{1-\mathrm{D}:} \quad Z_0^{\parallel} = -\frac{2ikZ_0}{b}\int_0^{\infty} \kappa |\tilde{h}(\kappa)|^2 d\kappa$$

$$\text{where} \quad \tilde{h}(k) = \frac{1}{2\pi}\int_{-\infty}^{\infty} h(z)e^{-ikz}dz$$

$$\underline{2-\mathrm{D}:} \quad Z_0^{\parallel} = -\frac{4ikZ_0}{b}\sum_{m=-\infty}^{\infty}\int_{-\infty}^{\infty}\frac{\kappa^2}{\sqrt{\kappa^2 + m^2/b^2}}|\tilde{h}_m(\kappa)|^2 d\kappa$$

$$\text{where} \quad \tilde{h}_m(k) = \frac{1}{(2\pi)^2}\int_0^{2\pi} d\theta \int_{-\infty}^{\infty} dz\, h(z,\theta)e^{-ikz-im\theta} \qquad (20)$$

Eq.(20) can be used to calculate the impedance of a tapered discontinuity. Note that the impedance is quadratic in the height of the small obstacle. The impedance is the same whether the wall bulges into or out of the pipe region.

Homework

Calculate the broad-band low-frequency impedance $Z_0^{\parallel}(\omega)$ for the beam pipe discontinutiy as shown below.

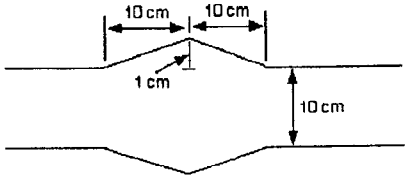

Small obstacles A special class of calculation applies when there is a small obstacle on the vacuum chamber wall. Using a theory developed by Bethe, one obtains, for low frequencies (ϕ is the azimuthal angle of the obstable relative to

the direction of the wake force being considered), a purely inductive impedance

Impedances	Wake functions
$Z_0^{\parallel} = -i\frac{\omega Z_0}{c}\frac{\alpha}{4\pi^2 b^2}$	$W_0' = -Z_0 c\frac{\alpha}{4\pi^2 b^2}\,\delta'(z)$
$Z_1^{\perp} = -i\frac{Z_0\alpha}{\pi^2 b^4}\cos\phi$	$W_1 = -Z_0 c\frac{\alpha}{\pi^2 b^4}\cos\phi\,\delta(z)$

(21)

The parameter α is related to the electric polarizability and magnetic susceptibility of the obstacle in the Bethe theory, and is a parameter (dimensionality = L^3) determined by the geometry of the obstacle. For examples,

$$\alpha = \begin{cases} \frac{2a^3}{3} & \text{circular hole of radius } a \\ \frac{\pi d^4[\ln(4a/d)-1]}{3a} & \text{elliptical hole with major radius } a \text{ along the pipe and minor radius } d \ll a \\ w^3(0.1814 - 0.0344\frac{w}{L}) & \text{rectangular slot of length } L \text{ and width } w \ll L \\ w^3(0.1334 - 0.0500\frac{w}{L}) & \text{rounded-end slot of length } L \text{ and width } w \ll L \\ \pi a^3 & \text{half spherical protrusion of radius } a \\ \frac{2\pi h^3}{3[\ln(2h/a)-1]} & \text{circular protrusion with height } a \ll h \end{cases} \tag{22}$$

The first four results apply when the pipe wall thickness is much smaller than the size of the small obstacle. If that is not the case, the value of α would be reduced by a multiplicative factor of about 0.6.

Trapped modes A small indent of the vacuum chamber wall out of the beam pipe region can contribute a sharp impedance, corresponding to a weakly trapped mode whose field pattern extends over a large distance over the indent. Consider a ring-shaped indent of cross-section area A in an axi-symmetric beam pipe. The impedance resonant frequency is located slightly below the TM_{01} pipe

cut-off frequency $\omega_{01} = x_{01}c/b$ by an amount

$$\Delta\omega_{01} = \omega_{01}\frac{x_{01}^2}{2}\left(\frac{A}{b^2}\right)^2 \tag{23}$$

where $x_{01} = 2.405$ is the first root of Bessel function $J_0(x)$. When the wall has a slight resistivity, the mode damps with damping rate $\gamma_{01} = \omega_{01}\delta_{\text{skin}}/(2b)$, where δ_{skin} is the skin depth. The trapped mode disappears when $\gamma_{01} > \Delta\omega_{01}$. Otherwise, it leads to a sharp longitudinal impedance with the shunt impedance

$$R_{01} = \frac{4Z_0 x_{01}A^3}{\pi\delta_{\text{skin}}b^5 J_1^2(x_{01})}, \qquad J_1(x_{01}) = 0.519 \tag{24}$$

Homework

Does the ring-shaped indentation in the following figure allow a trapped mode? Consider a copper beam pipe.

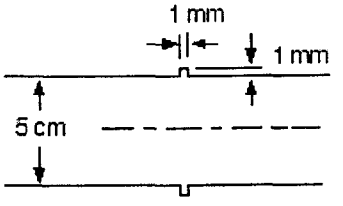

Figure 5: A possibility of trapped mode.

Rough metallic surface The result for slowly varying surface and the result for small obstacles can also be used to estimate the low-frequency inductive impedance of a rough metallic surface provided the surface characteristics are known. A long pipe with rough wall surface behaves like a periodic array of small pill-boxes, and a resonator-type contribution like (17) will also be present.

4 Parasitic Heating

The energy change (parasitic loss) of a bunch of charge q and normalized line density $\lambda(t)$, traversing a structure with longitudinal impedance $Z_0^{\parallel}$ is given by

$$\Delta\mathcal{E} = -\kappa^{\parallel} q^2 \tag{25}$$

where $\kappa^{\parallel}$ is the *loss factor*, in units of V/pC,

$$\kappa^{\parallel}(\sigma) = \frac{1}{\pi}\int_0^{\infty} d\omega\, \mathrm{Re}Z_0^{\parallel}(\omega)\,|\tilde{\lambda}(\omega)|^2 \tag{26}$$

where $\sigma = \sigma_z/\beta c$ is the rms beam bunch length in sec. For a gaussian bunch, $\lambda = e^{-t^2/2\sigma^2}/(\sqrt{2\pi}\sigma)$, $\tilde{\lambda}(\omega) = e^{-\omega^2\sigma^2/2}$.

Only the real part of the impedance contributes to the parasitic loss. Inductive impedances and the space charge impedance do not introduce a net power loss to the beam. Energy loss by particles at the head of the bunch is recovered by particles in the tail of the bunch (see e.g., Eq.(35) later).

One can also write the loss factor in terms of the wake function. For a gaussian bunch,

$$\kappa^{\parallel} = \frac{1}{2\sqrt{\pi}\,\sigma}\int_{-\infty}^{0} \frac{dz}{c}\, W_0'(z)\, e^{-z^2/4\sigma^2c^2} \tag{27}$$

Resistive wall A resistive wall impedance gives

$$\frac{\kappa^{\parallel}(\sigma)}{L} = \frac{\Gamma(\frac{3}{4})c}{4\pi^2 b\sigma_z^{3/2}}\left(\frac{Z_0}{2\sigma_c}\right)^{1/2}, \qquad \Gamma(\frac{3}{4}) = 1.225 \tag{28}$$

Pill-box cavity For a bunch traversing a pill-box cavity, $\kappa^{\parallel}$ is given by a sum over cavity modes up to the cut-off frequency, plus a contribution from the diffraction model impedance. Each of the cavity modes contributes a resonator

impedance, and each resonator impedance contributes

$$\kappa^{\parallel} \approx \begin{cases} \frac{\omega_r R_s}{2Q_r} e^{-\omega_r^2 \sigma^2} & \text{high-}Q\text{ resonator} \\ \frac{\omega_r R_s}{2Q_r} & \text{low-}Q\text{ resonator, short bunch } \omega_r \sigma \ll 1 \\ \frac{R_s}{4\sqrt{\pi} Q_r^2 \omega_r^2 \sigma^3} & \text{low-}Q\text{ resonator, long bunch } \omega_r \sigma \gg 1 \end{cases} \tag{29}$$

The contribution from the high frequency diffraction impedance is

$$\kappa^{\parallel} \approx \frac{\Gamma(\frac{1}{4}) Z_0}{4\pi^{5/2} b} \sqrt{\frac{cg}{\sigma}} \tag{30}$$

For a single bunch in a circular accelerator, the integral in Eq.(26) is replaced by an infinite sum,

$$\kappa^{\parallel}(\sigma) = \frac{\omega_0}{2\pi} \sum_{p=-\infty}^{\infty} Z_0^{\parallel}(p\omega_0) \, |\tilde{\lambda}(p\omega_0)|^2 \tag{31}$$

For short bunches in large machines ($\omega_0 \ll 1/\sigma$), the sum can be replaced by an integral, and the difference between single passes and multiple passes disappears as it should.

Homework

Consider a storage ring with smooth resistive pipe. Let circumference $C = 100$ m, $b = 5$ cm, $N = 10^{11}$ protons (ignore synchrotron radiation), $\sigma_z = 1$ cm, $\sigma_c = 3.5 \times 10^7 \Omega^{-1} m^{-1}$ (aluminum). Let there be one single cavity structure in the ring with $g = 10$ cm, which has 6 trapped HOMs with $R/Q = 60\,\Omega$ each. (1) Estimate the parasitic heating power due to resistive wall. (2) Estimate the parasitic heating power due to the cavity HOMs below cut-off. (3) Estimate the parasitic heating power due to the cavity above cut-off. (4) How are the above heating powers distributed around the accelerator? What if the pipe is made of stainless steel? (5) Do we need water cooling for the pipe? Do we need water cooling for the rf cavity due to the parasitic heating?

Hints

(2) Since $\omega_{\text{cut-off}} \approx c/b$, the trapped modes most likely will have $\omega_R \ll c/\sigma_z$. This means we should use the short bunch formula in Eq.(29). Let the 6 trapped modes have $\omega_R = (1, 5/6, 4/6, 3/6, 2/6, 1/6)c/b$, add up the heating due to the 6 modes. This heating is trapped by the cavity.

(3) Use diffraction model. This power propagates down the two directions from the cavity.

(4) First estimate the attenuation length of the untrapped modes in (3). Let this power dissipation be given by $e^{-2\beta z}$, then very roughly, $\beta \approx c/(4\pi b \sigma_c \delta_{\text{skin}})$. Is the untrapped wave absorbed near the cavity, or does it propagate around the ring more or less evenly?

(5) Without water cooling, the heated area will have to cool by black body radiation. The black body radiation per meter is given by $dQ/dt = -(2\pi b)\pi^2 k_B^4 T^4/(15\hbar^3 c^2)$. Therefore, in equilibrium, $dQ_{\text{parasitic heating}}/dt = (2\pi b)\pi^2 k_B^4 [T^4 - T_0^4]/(15\hbar^3 c^2)$ where T_0 is the room temperature. Estimate the equilibrium temperature T at the cavity and on the beam pipe around the ring to see if water cooling is needed.

5 Collective Effects in High Energy Linacs

Energy variation along the bunch length As a beam bunch travels down the linac, the longitudinal wake induces an energy variation along the length of

the bunch (consult Eq.(4) for the wake force),

$$\begin{aligned} -\Delta E(z) &= Ne^2 \int_z^\infty dz' \lambda(z')\, W_0'(z-z') \\ &= \frac{Ne^2}{2\pi} \int_{-\infty}^\infty d\omega\; e^{i\omega z/c}\, Z_0^{\parallel}(\omega)\, \tilde{\lambda}(\omega) \end{aligned} \tag{32}$$

This variation can be compensated for by properly phasing the bunch center relative to crest of the acceleration rf. The total energy change of the beam is given by

$$\Delta \mathcal{E} = N \int_{-\infty}^\infty dz\, \Delta E(z)\, \lambda(z) \tag{33}$$

which is just the $\Delta\mathcal{E}$ in Eq.(25). A rough order-of-magnitude estimate of the head-tail energy split is

$$-\Delta E \sim \frac{Ne^2}{2} W_0' \tag{34}$$

provided one has an estimate of the magnitude of W_0'.

For longitudinally gaussian bunch of charge Ne, rms length σ_z, and transverse radius a, travelling in cylindrical, perfectly conducting beam pipe of radius b, the space charge wake-induced energy variation along the bunch is

$$\frac{\Delta E(z)}{L} = \frac{1}{4\pi\epsilon_0} \sqrt{\frac{2}{\pi}} \frac{Ne^2}{\gamma^2 \sigma_z^2} \left(\ln \frac{b}{a} + \frac{1}{2} \right) \frac{z}{\sigma_z} \exp(-z^2/2\sigma_z^2) \tag{35}$$

The total loss of the beam is zero, as mentioned before, because the space charge impedance is purely imaginary.

For a resistive wall,

$$\begin{aligned} \frac{\Delta E(z)}{L} &= \frac{1}{4\pi\epsilon_0} \frac{Ne^2}{4b\sigma_z^{3/2}} \sqrt{\frac{2}{Z_0 \sigma_c}} f\left(\frac{z}{\sigma_z}\right) \\ f(u) &= -|u|^{3/2} e^{-u^2/4} \left[(I_{-1/4} - I_{3/4}) \mathrm{sgn}(u) - I_{1/4} + I_{-3/4} \right] \end{aligned} \tag{36}$$

where $I_{\pm 1/4}$ and $I_{\pm 3/4}$ are modified Bessel functions evaluated at $u^2/4$. See Fig.6.

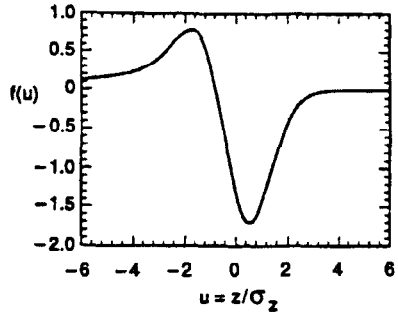

Figure 6: Function $f(u)$ in Eq.(36).

Homework

Estimate the wake-induced energy variation for the SLAC linac. Let $N = 5 \times 10^{10}$, and $L = 3000$ m. Model the SLAC linac cavities as an array of pill-boxes whose dimensions are comparable to the pipe radius $b = 1$ cm. What is the head-tail $\Delta E/E$-split of the beam when the beam reaches 50 GeV at the end of the linac if we do not compensate for this energy variation by properly phasing the rf?

Hints

Use Eq.(34), with a rough estimate of W_0' per cavity given by Eq.(15). The total number of cavities is about L/b.

Transverse beam break-up The equation of motion is (consult Eq.(4) for the wake force)

$$\frac{d}{ds}\left(E(s)\frac{d}{ds}x(z,s)\right)+E(s)k^2(s)x(z,s)=\frac{Ne^2}{L}\int_z^\infty \lambda(z')W_1(z'-z)x(z',s)dz' \tag{37}$$

Given the wake function $W_1(z)$ of the entire linac (of length L), the longitudinal bunch distribution $\lambda(z)$, the energy acceleration $E(s)$ and betatron focussing $k(s)$, Eq.(37) is to be solved for the betatron motion $x(z,s)$ as a function of s for a particle located at position z relative to the bunch center.

For uniform $\lambda = 1/\ell$ (ℓ is total length of bunch), $W_1(z) = W_1' z$, and when the variations of E and k are adiabatic, the asymptotic solution is

$$\frac{\text{final amplitude}}{\text{initial amplitude}} \approx \sqrt{\frac{E(0)k(0)}{E(L)k(L)}}\,\frac{\eta^{-1/6}}{\sqrt{6\pi}}\exp\left(\frac{3\sqrt{3}}{4}\eta^{1/3}\right) \quad (\eta \gg 1) \tag{38}$$

where

$$\eta(z)=\frac{Ne^2W_1'}{L\ell}\left(z-\frac{\ell}{2}\right)^2\int_0^L\frac{ds}{E(s)k(s)}$$

The bunch head has $z = \ell/2$ and thus $\eta = 0$. The exponential growth in Eq.(38) illustrates the *beam break-up instability*. This problem is usually cured by the *BNS damping*.

Homework

Estimate how potentially serious is the beam break-up instability problem for the SLAC linac (no BNS damping). Let $E(s)$[GeV] = $1.2+0.017s$[m], $k(s) = 0.06$/m, $N = 5\times10^{10}$, $\ell = 2$ mm, $b = 1$ cm, and $L = 3000$ m.

Hint

Use Eq.(15) for W_1 per cavity. Our model then corresponds to taking $W_1' \sim (W_1/b) \times (L/b)$. Consider the particle at the tail of the bunch by taking $z = -\ell/2$.

BNS damping BNS damping is accomplished by having the particles at the tail of the bunch being focussed more strongly than particles at the head of the bunch. The stronger focusing balances out the defocusing effect of the transverse wake. The net result is that the wake-induced emittance growth is minimized. The condition for this to occur is called the *autophasing condition.* In case of uniform acceleration and uniform betatron focusing, it reads

$$\frac{\Delta k(z)}{k} = -\frac{Ne^2}{2k^2 L E_f} \ln\frac{E_f}{E_i} \int_z^\infty \lambda(z') W_1(z - z') dz' \tag{39}$$

An order-of-magnitude estimate of the needed BNS focusing is given by

$$\frac{\Delta k}{k} \approx -\frac{Ne^2 W_1(\ell)}{4k^2 L E_f} \ln\frac{E_f}{E_i} \tag{40}$$

where $W_1(\ell)/L$ is the transverse wake function per unit length seen by a particle at the tail of the bunch.

Homework

Estimate the BNS focusing needed for the SLAC linac.

Hint

Using Eq.(15) to obtain $W_1(\ell) \sim (1/b^2) \times (L/b) \times (\ell/b)$, we obtain $\Delta k/k \sim (Ne^2 \ell / 4k^2 E_f b^4) \ln(E_f/E_i)$.

Multibunch transverse dynamics Consider a beam with n_B equally-populated, equally-spaced bunches, each with charge Ne. Motion of each bunch is

affected by the transverse wake left behind by the previous bunches (or the same bunch in previous turns). The analysis is similar to that of the BBU effect within a single bunch. The difference is that here W_1 is dominated by one or a few resonators having large shunt impedances. In case of a single isolated resonator, the amplitude blowup factor of the last bunch takes a form $\sim e^{\sqrt{\eta}}$ where

$$\eta = n_B N e^2 \frac{R_s \omega_r}{Q} \int_0^L \frac{ds}{E(s)k(s)} \gg 1 \tag{41}$$

The condition for tolerable emittance growth due to multi-bunch transverse wake is roughly given by $\eta \lesssim 1$.

6 Robinson Instability

Instability mechanisms in a linac are comparatively simple because of the absence of synchrotron oscillation. In a circular accelerator, synchrotron oscillation plays a critical role. (Fortunately, the role is often a stabilizing one.) The most basic collective instability in a circular accelerator is the Robinson instability.

Single-bunch, point-charge beam Consider a beam with a single bunch executing synchrotron motion in a circular accelerator. First let the bunch be represented as a point charge Ne without any internal structure. Given the impedance $Z_0^{\parallel}(\omega)$ of the accelerator, the stability of this beam is analyzed by assuming the beam is executing a collective motion as $z(t) \sim e^{-i\Omega t}$. The key quantity to be calculated is the *collective mode frequency* Ω. It is a complex quantity directly related to the impedance. The real part of Ω is the perturbed

synchrotron oscillation frequency of the collective beam motion, while the imaginary part gives its growth rate (or damping rate if negative). The result of the growth rate is

$$\tau^{-1} = \mathrm{Im}(\Omega - \omega_s) = \frac{Ne^2\eta}{2ET_0^2\omega_s} \sum_{p=-\infty}^{\infty} (p\omega_0 + \omega_s)\mathrm{Re}Z_0^{\parallel}(p\omega_0 + \omega_s) \qquad (42)$$

where η is the momentum slippage factor, ω_0 is the revolution angular frequency, $T_0 = 2\pi/\omega_0$ is the revolution period, ω_s is the unperturbed synchrotron oscillation frequency. Note that it is the real part of the impedance that contributes to the instability growth rate. A space charge impedance causes a mode frequncy shift, but not an instability.

Eq.(42) applies to any impedance. The largest impedance to be considered is the resonator impedance of the fundamental cavity mode, which has $\omega_R \approx h\omega_0$ (h = integer is the *harmonic number*). The only significant contributions to the growth rate come from two terms in the summation, namely $p = \pm h$,

$$\tau^{-1} \approx \frac{Ne^2\eta h\omega_0}{2ET_0^2\omega_s}\left[\mathrm{Re}Z_0^{\parallel}(h\omega_0 + \omega_s) - \mathrm{Re}Z_0^{\parallel}(h\omega_0 - \omega_s)\right] \qquad (43)$$

Beam stability requires $\tau^{-1} \leq 0$. That is, the real part of the impedance must be lower at frequency $h\omega_0 + \omega_s$ than at frequency $h\omega_0 - \omega_s$ if $\eta > 0$ (above transition), and the other way around if $\eta < 0$ (below transition). This condition implies the *Robinson criterion* that, above transition, the resonant frequency ω_R of the fundamental cavity mode should be slightly detuned downwards from an exact integral multiple of ω_0. Below transition, stability requires ω_R be slightly higher than $h\omega_0$. In the figure below, (a) is stable above transition, while (b) is stable below transition.

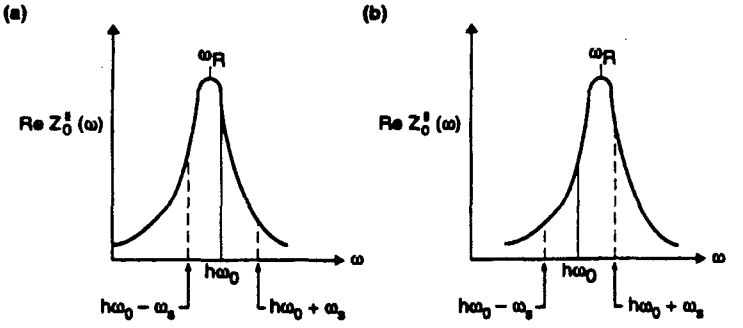

After properly tuning the fundamental rf cavity mode, one should consider the contributions from the higher rf modes, paying attention to accidentally landing the frequencies $p\omega_0$ for some integer p on the wrong side of some higher order impedance peak. Sometimes it becomes necessary to damp the higher order modes of the rf to avoid excessive instability growth rates.

Multi-bunch beam Eq.(42) is restricted because (i) it applies to a beam with only one bunch, and (ii) the beam bunch is a point-charge. Consider a beam with n_B evenly-spaced, equally-populated bunches. This time also consider bunches with finite length to allow internal structure of the mode patterns within each bunch. There are now a large number of collective modes in our problem, and the mode frequency Ω depends on the mode being considered. A mode is now specified by two mode indices μ and ℓ, where $\mu = 0, 1, 2, ..., (n_B - 1)$ is the multi-bunch mode number, and ℓ is the internal bunch structure mode number ($\ell = 1$ dipole, $\ell = 2$ quadrupole, etc.). The growth rate is found to be

$$\frac{1}{\tau^{(\ell,\mu)}} = \mathrm{Im}(\Omega^{(\ell,\mu)} - \ell\omega_s) = \frac{2n_B N e^2 \eta c^2}{ET_0^2 \omega_s \hat{z}^2}\, \ell \sum_{p=-\infty}^{\infty} \frac{\mathrm{Re}Z_0^{\parallel}(\omega')}{\omega'}\, J_\ell^2\left(\frac{\omega'\hat{z}}{c}\right) \qquad (44)$$

where N is the number of particles per bunch, $\omega' = pn_B\omega_0 + \mu\omega_0 + \ell\omega_s$. In deriving Eq.(44), it has been assumed that the unperturbed bunch distribution is described by a "waterbag model". The full extent of the bunch length is $2\hat{z}$.

The lowest bunch structure mode has $\ell = 1$ (dipole). For short bunches with $\omega'\hat{z}/c \ll 1$, and for $n_B = 1$, Eq.(44) reduces to Eq.(42). On the other hand, Eq.(44) also applies to higher order modes $\ell > 1$ and arbitrary bunch length $\hat{z}$. In particular, the fundamental rf mode contributes to a Robinson growth rate for the ℓth beam mode,

$$\begin{aligned}\frac{1}{\tau^{(\ell,0)}} &= \frac{\ell}{(\ell!)^2}\left(\frac{h\omega_0\hat{z}}{2c}\right)^{2\ell-2}\frac{n_B N e^2\eta h\omega_0}{2ET_0^2\omega_s} \\ &\quad\times[\mathrm{Re}\,Z_0^{\parallel}(h\omega_0+\ell\omega_s) - \mathrm{Re}Z_0^{\parallel}(h\omega_0-\ell\omega_s)] \qquad (45)\end{aligned}$$

It follows that the Robinson stability criterion for the $\ell = 1$ mode also stabilizes the $\ell > 1$ modes. The higher order Robinson growth rates, however, drop off rapidly with increasing ℓ if the bunch length is much less than the rf wavelength.

Note that h is necessarily an integral multiple of n_B, thus only the $\mu = 0$ multi-bunch mode is affected by the fundamental rf mode, and the growth rate is directly proportional to n_B. Other multi-bunch modes ($\mu \neq 0$) must be considered when studying the effects of the higher order rf modes.

7 Transverse Robinson Instability

Robinson instability has a transverse counterpart. Basically the same physical mechanism applies when we consider the transverse beam motion driven by the transverse impedance. Letting $y \propto \exp(-i\Omega t)$, the instability growth rate is

found to be

$$\tau^{-1} = \mathrm{Im}(\Omega - \omega_\beta) \approx -\frac{Ne^2c}{2ET_0^2\omega_\beta} \sum_{p=-\infty}^{\infty} \mathrm{Re}Z_1^\perp(p\omega_0 + \omega_\beta) \qquad (46)$$

where $Z_1^\perp$ is the total impedance around the accelerator circumference. Only the real part of the impedance contributes to the instability growth rate. The space charge impedance does not cause instability of the Robinson type.

A transverse Robinson instability occurs when $\mathrm{Re}Z_1^\perp(\omega)$ contains sharp resonant peaks. If a resonant frequency ω_R is close to $h\omega_0$ for some integer h, then

$$\tau^{-1} \approx -\frac{Ne^2c}{2ET_0^2\omega_\beta} \left[\mathrm{Re}Z_1^\perp(h\omega_0 + \Delta_\beta\omega_0) - \mathrm{Re}Z_1^\perp(h\omega_0 - \Delta_\beta\omega_0)\right] \qquad (47)$$

where Δ_β is the non-integer part of the betatron tune $\nu_\beta = \omega_\beta/\omega_0$ and we have chosen $-1/2 < \Delta_\beta < 1/2$. A positive Δ_β means ν_β is above an integer; a negative Δ_β means ν_β is below an integer. For stability, ω_R should be slightly above $h\omega_0$ if $\Delta_\beta > 0$ and below $h\omega_0$ if $\Delta_\beta < 0$. The stability criterion of the transverse Robinson instability does not depend on whether the accelerator is operated above or below transition. Instead, it depends on whether the betatron tune is above or below an integer.

Homework

Find the transverse Robinson instability growth rate for the case $N = 10^{11}$, $R_S = 40$ MΩ/m^2, $Q = 2000$, $E = 1$ GeV (electron beam), $\omega_0 = 9.4 \times 10^6$ s^{-1}, $\nu_\beta = 6.05$, $h = 518$, and $(\omega_R - h\omega_0)/\omega_0 = \pm h/2\sqrt{3}Q$ (the worst case).

Like its longitudinal counterpart, to control the transverse Robinson instability, it is often necessary to de-Q the transverse higher order modes of the rf

cavities by either passively or actively removing their field energies. Unlike its longitudinal counterpart, the transverse Robinson instability does not have the strong damping provided by the fundamental rf cavity mode (assumed properly tuned), which makes it more of a serious concern.

In case of a broad-band impedance (short-ranged wake field), the summation over p can be approximated by an integral over p. It then follows from Eq.(46) and the fact that $\mathrm{Re}Z_1^\perp$ is an odd function of ω that $\tau^{-1} = 0$. Broad-band impedances therefore do not cause transverse Robinson instability, a situation similar to the longitudinal case. However, as will be explained later, a broad-band impedance does cause an instability when the betatron frequency of a particle is not a constant, as assumed so far, but depends on its relative energy deviation $\delta = \Delta E/E$.

Resistive wall instability Eq.(46) also gives the instability growth rate for an accelerator with a resistive vacuum chamber. Substituting Eq.(8) into Eq.(46), we obtain

$$\begin{aligned} \tau^{-1} &\approx -\frac{Ne^2c^2}{b^3 E\omega_\beta T_0\sqrt{\pi\sigma_c\omega_0}}\, f(\Delta_\beta) \qquad (48) \\ f(\Delta_\beta) &= \frac{1}{\sqrt{2}}\sum_{p=-\infty}^{\infty}\frac{\mathrm{sgn}(p+\Delta_\beta)}{|p+\Delta_\beta|^{1/2}} \end{aligned}$$

when $|\Delta_\beta| \ll 1$, the $p = 0$ term dominates in the summation for $f(\Delta_\beta)$.

The function $f(\Delta_\beta)$ is positive (so that $\tau^{-1} < 0$ and the beam is stable) if $0 < \Delta_\beta < 1/2$, and negative if $-1/2 < \Delta_\beta < 0$. This means one should choose the betatron tune above an integer to assure stability against the resistive wall instability. However, because the resistive wall instability is usually rather weak

(Very large storage rings are an exception because they have small ω_0, and according to Eq.(48), can potentially have large growth rates.), a small spread of betatron tune of the particles in the beam will stabilize the beam even if the betatron tune is below an integer (see Landau damping later).

Homework

Estimate the transverse resistive wall instability growth rate for the case $N = 10^{11}$, $b = 5$ cm, $E = 1$ GeV (electron beam), $\nu_\beta = 5.9$ (below an integer, therefore the beam is unstable), $\omega_0 = 9.4 \times 10^6$ s^{-1}, and $\sigma = 3 \times 10^{17}$ s^{-1}.

8 Strong Head-Tail Instability

The strong head-tail instability (also called *transverse mode coupling* instability or *transverse turbulence* instability) is the circular accelerator's counterpart of the dipole beam breakup in a linac. The difference from the linac case is that now the beam particles execute synchrotron oscillations, thus constantly changing their relative longitudinal positions with a slow synchrotron frequency ω_s.

In the discussion of transverse Robinson instability, it was stated that a broad-band impedance (short ranged wake) does not cause an instability. However, this is only true when one ignores coupling between the "azimuthal modes" of the beam motion. The dimensionless parameter that describes the strength of the mode coupling is given by

$$\Upsilon = -\frac{\pi N e^2 W_1 c^2}{4EC\omega_\beta \omega_s} \tag{49}$$

where $W_1 < 0$ is the short-range wake function (integrated over the accelerator

circumference C), assumed to be constant over the bunch length.

For low beam intensities, $\Upsilon \ll 1$, mode coupling is negligible and adjacent azimuthal modes have their frequencies well separated by ω_s. The beam is stable for short-ranged wake, as we discussed in the context of Robinson instability. As beam intensity increases, however, mode coupling becomes significant. As the mode frequencies shift by amounts comparable to ω_s, adjacent azimuthal mode frequencies may merge into each other, and the beam becomes unstable even with a short-range wake. This is called the strong head-tail instability. The threshold of this instability occurs at

$$\Upsilon_{\text{th}} = 2 \tag{50}$$

The reason it is called *strong* head-tail instability is that once the threshold is exceeded, the instability tends to grow very fast.

Homework

The strong head-tail instability is one of the cleanest instabilities to observe in electron storage rings. The instability threshold observed at PEP occurred when $N_{\text{th}} = 6.4 \times 10^{11}$, $\omega_\beta/\omega_0 = 18.19$, $\omega_s/\omega_0 = 0.044$, $E = 14.5$ GeV, and $\omega_0 = 0.86 \times 10^6$ s^{-1}. By relating these parameters to $\Upsilon_{\text{th}} = 2$, estimate the wake function W_1 and the transverse impedance $Z_1^\perp$ for PEP. Take a beam pipe radius $b = 5$ cm. Once $Z_1^\perp$ is found, relate it to give an estmate of $Z_0^\parallel/n$.

Hint

To estimate $Z_1^\perp$ once W_1 is found, use $Z_1^\perp \approx -bW_1/c$.

9 Head-Tail Instability

In our analysis of the strong head-tail instability, we assumed that the betatron and the synchrotron motions are decoupled. In doing so, we have ignored an important instability known as the head-tail instability.

The betatron oscillation frequency of a particle depends on $\delta = \Delta E/E$ of the particle through the chromaticity parameter ξ,

$$\omega_\beta(\delta) = \omega_\beta(1 + \xi\delta) \tag{51}$$

As we will see, in order to avoid head-tail instability, ξ must have a definite sign. The main reason for introducing sextupoles in circular accelerators is in fact to control ξ.

Because of a nonzero chromaticity, the betatron phase of a particle is modulated by the longitudinal position z of the particle. The modulation is slow and weak, but is sufficient to drive the head-tail instability. The magnitude of this phase modulation is specified by the *head-tail phase*,

$$\chi = \frac{\xi\omega_\beta\hat{z}}{c\eta} \tag{52}$$

with $\pm\hat{z}$ the extent of the bunch length. For example, an electron accelerator with $\eta = 0.003$, $\xi = 0.2$, $\hat{z} = 3$ cm, and $\omega_\beta = 1.4 \times 10^7$ s^{-1}, would have $\chi \approx 2\pi \times 0.016$.

The strong head-tail instability is a threshold effect. It occurs when the beam current exceeds a certain critical value. Once the threshold is exceeded, the instabilty is very strong. In contrast, the head-tail instability is not a threshold effect. It is unstable even for weak beam currents, although the growth rate is

slow. Note however that the *same* transverse impedance (typically broad-band) drives both the head-tail and the strong head-tail instabilities.

Taking into account of the chromaticity effect, the transverse instability growth rate for the ℓth mode ($\ell = 0$ for monopole, $\ell = 1$ for dipole, etc.) is found to be

$$\frac{1}{\tau^{(\ell)}} = \mathrm{Im}(\Omega - \omega_\beta - \ell\omega_s) \approx -\frac{Ne^2c}{2ET_0^2\omega_\beta} \sum_{p=-\infty}^{\infty} \mathrm{Re}Z_1^\perp(\omega')\, J_\ell^2\left(\frac{\omega'\hat{z}}{c} - \chi\right) \qquad (53)$$

where $\omega' = p\omega_0 + \omega_\beta + \ell\omega_s$. Note how the head-tail phase appears in shifting the beam spectrum which is then convoluted with the impedance when summing over p. Eq.(53) is a rather general result. For example, When $\ell = 0$, $\chi = 0$, and $\hat{z} = 0$, it reduces to Eq.(46). However, it did assume an "air-bag model" for the unperturbed longitudinal beam distribution, although the impedance is left aribitrary.

When $\chi \ll 1$, Eq.(53) gives the head-tail instability growth rate, to first order in χ,

$$\frac{1}{\tau^{(\ell)}} \approx \frac{Ne^2c}{\pi ET_0\omega_\beta}\, \chi \int_0^\infty d\omega\ \mathrm{Re}\, Z_1^\perp(\omega)\, J_\ell\left(\frac{\omega\hat{z}}{c}\right) J_\ell'\left(\frac{\omega\hat{z}}{c}\right) \qquad (54)$$

where we have considered a broad-band impedance, so that the summation in p can be replaced by an integral.

For the case of a constant wake function ($W_1(z)$ is independent of z, $W_1 < 0$), Eq.(54) gives

$$\frac{1}{\tau^{(\ell)}} = -\frac{Ne^2cW_1}{ET_0\omega_\beta}\, \chi\, \frac{2}{\pi^2(4\ell^2 - 1)} \qquad (55)$$

According to Eq.(55), the $\ell = 0$ mode is unstable when $\xi/\eta < 0$, while the $\ell \geq 1$ modes are unstable when $\xi/\eta > 0$. We conclude from this that the only

value of ξ that assures a stable beam is $\xi = 0$. However, the $\ell = 0$ growth rate is the strongest. The presence of some stabilizing mechanisms (such as Landau damping, or radiation damping in the case of circular electron accelerators) therefore leads us to choose slightly positive values for ξ for operation above transition ($\eta > 0$), and slightly negative ξ below transition ($\eta < 0$).

The head-tail growth rate provides another way to measure the transverse impedance of an accelerator. To do so, ξ is made slightly positive (above transition), a beam centroid motion is excited by a kicker, and its subsequent damped motion is observed. Before applying Eqs.(54) or (55), make sure that $\xi \ll 1$. Usually, radiation damping is much weaker than the head-tail damping. Otherwise the contribution from radiation damping has to be subtracted out from the measured damping rate.

Homework

It was observed in the electron storage ring SPEAR I that the head-tail damping time is 1 ms under the conditions $I = 20$ mA, $E = 1.5$ GeV, $\xi = 0.67$, $\hat{z} = 13$ cm, $\eta = 0.037$, $C = 240$ m, $b = 5$ cm. Estimate the magnitudes of W_1, $Z_1^{\perp}$, and $Z_0^{\parallel}/n$.

10 Landau Damping

So far, we have ignored the important effect of Landau damping. Landau damping occurs when there is a sufficient spread in particles' natural oscillation frequencies. Table below gives the natural frequencies needed by the Landau damping mechanism in order to damp the respective instabilities.

	Bunched beam	Unbunched beam
Longitudnal	synchrotron frequency ω_s	revolution frequency ω_0
Transverse	betatron frequency ω_β	betatron frequency ω_β

Consider an unbunched beam executing longitudinal or transverse oscillation. Let the frequency spectrum $\rho(\omega)$ be normalized to unity (ω is the frequency relevant to the Landau damping mechanism, and is given in the table above), and be centered around $\bar{\omega}$ with spread $S \ll \bar{\omega}$. The strength of Landau damping depends on $\rho(\omega)$.

Transverse microwave instability Consider an unbunched beam executing a transverse oscillation with dipole perturbation $\propto e^{-i\Omega t + in(s/R)}$ where n is the mode number. Whether the beam is stable is determined by the following steps:

(i) Given the impedance, one first calculates the complex mode frequency shift – its imaginary part is the instability growth rate – in the *absence* of Landau damping, designated with a subscript 0 (compare with Eq.(46)),

$$(\Delta\omega)_0 \equiv (\Omega - n\omega_0 - \bar{\omega})_0 = -\frac{Ne^2c}{2ET_0^2\omega_\beta} iZ_1^\perp(\bar{\omega} + n\omega_0) \tag{56}$$

where $\bar{\omega}$ is the center of the betatron frequency spectrum.

(ii) Given the spectral distribution $\rho(\omega)$, one calculates the *unperturbed beam transfer function*, which is a dimensionless function of Ω,

$$\text{BTF} = f(u) + ig(u) \tag{57}$$

where (PV means taking principal value)

$$u = (\omega_\beta + n\omega_0 - \Omega)/S$$

$$f(u) = S\,\mathrm{PV}\int d\omega \frac{\rho(\omega)}{\omega - \Omega}$$
$$g(u) = \pi S \rho(\Omega) \tag{58}$$

(iii) With Landau damping, the complex mode frequency Ω, for a mode which is at the edge of stability, is determined by the *dispersion relation*

$$-\frac{(\Delta\omega)_0}{S} = \frac{1}{\mathrm{BTF}} \tag{59}$$

To obtain boundary of stability: (a) trace the locus of the r.h.s. of Eq.(59) on a complex plane as u is scanned from $-\infty$ to ∞. This trace divides the complex plane into two regions, one contains the origin, the other doesn't. (b) Plot the l.h.s. of Eq.(59) as a single point on the same complex plane. (c) If this point lies in the region which contains the origin, the beam is stable; otherwise it is unstable. Fig.7 shows the stability region produced in step (b) for several spectral distributions. When the beam lies in the unstable region, the beam is said to have a *transverse microwave instability.*

A simplified stability boundary, as sketched in Fig.7(h), leads to the *Keil-Schnell criterion,*

$$|(\Delta\omega)_0| < \frac{1}{\sqrt{3}} S_{\frac{1}{2}} \tag{60}$$

where $S_{\frac{1}{2}}$ is the half width at half maximum of the frequency spectrum. Roughly speaking, when the instability growth rate or mode frequency shift (calculated in the absence of Landau damping) exceeds the beam frequency spread, one loses the protection of Landau damping, and the beam is most likely unstable.

Bunched beam

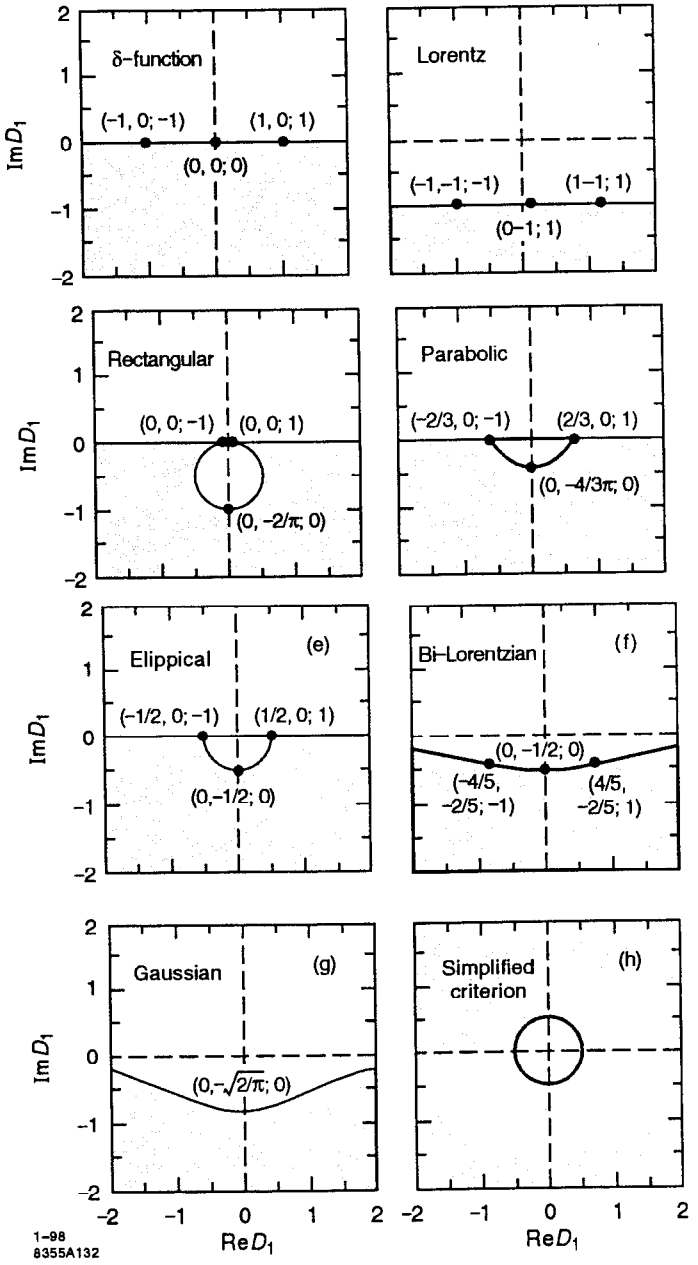

Figure 7: Stability diagram for transverse microwave instability for various beam spectra. Shaded regions are unstable.

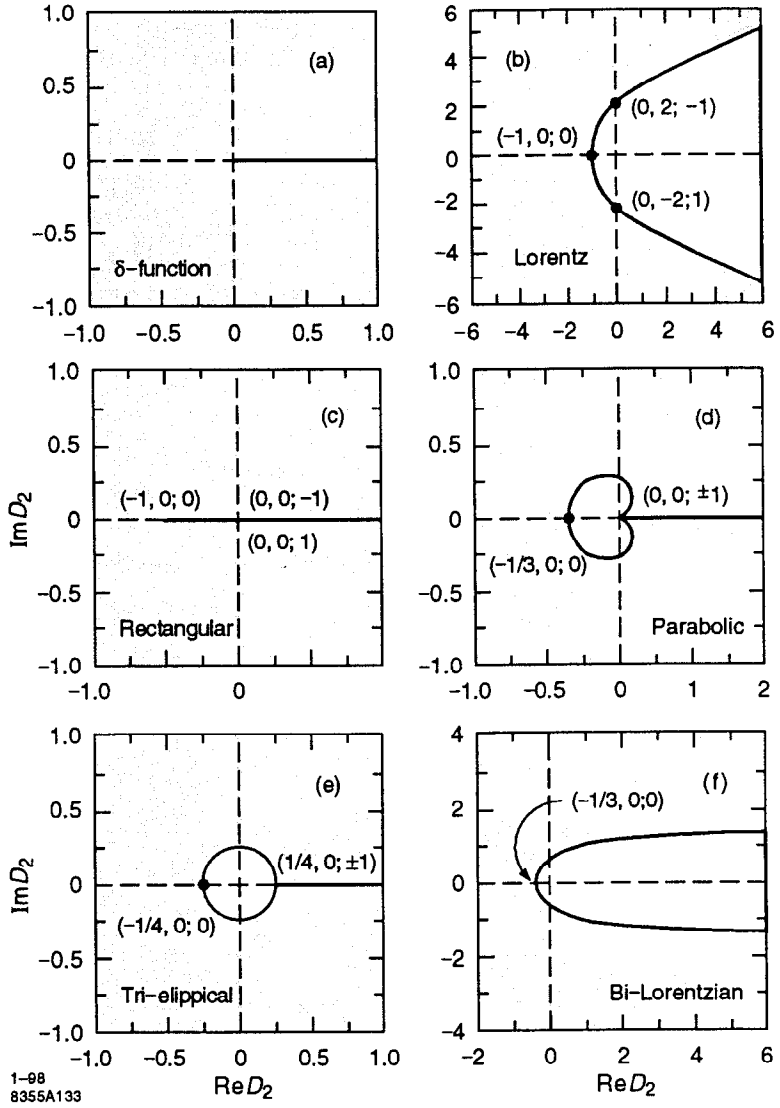

Figure 8: Stability diagram for longitudinal microwave instability for various beam spectra. Shaded regions are unstable.

The simplified stability criterion Eq.(60) applies to unbunched beams, but it can be applied to a bunched beam if one replaces the beam density N/C by the

peak local density of the bunched beam. This is called the *Boussard criterion.*

For a bunched beam whose length is smaller than the pipe radius b, the simplified criterion against transverse microwave instability reads

$$|Z_1^{\perp}| < Z_0 \frac{\pi E|\eta|\omega_\beta \Delta\delta_{\frac{1}{2}} \Delta z_{\frac{1}{2}}}{3Ne^2\omega_0 b} \tag{61}$$

Relating the longitudinal to the transverse impedance, it gives

$$\left|\frac{Z_0^{\parallel}}{n}\right| < Z_0 \frac{\pi E|\eta|\omega_\beta b\Delta\delta_{\frac{1}{2}} \Delta z_{\frac{1}{2}}}{6Ne^2c} = Z_0 \frac{\pi E\omega_\beta\omega_s b\Delta z_{\frac{1}{2}}^2}{6Ne^2c^2} \tag{62}$$

Longitudinal microwave instabilities Similar steps apply to the longitudinal microwave instability of an unbunched beam. The complex mode frequency shift in the absence of Landau damping is now given by

$$(\Delta\omega)_0^2 \equiv (\Omega - n\omega_0)_0^2 = i\frac{2\pi Ne^2 n\eta}{ET_0^3} Z_0^{\parallel}(n\omega_0) \tag{63}$$

Landau damping comes from a spread in ω_0, spectrum $\rho(\omega_0)$ with spread S around center $\bar{\omega}_0$. The dispersion relation is

$$\begin{aligned} \frac{(\Delta\omega)_0^2}{n^2S^2} &= \frac{1}{F(u) + iG(u)} \\ u &= (n\bar{\omega}_0 - \Omega)/(nS) \\ F(u) &= nS^2 \ \mathrm{PV}\int d\omega_0 \frac{\rho'(\omega_0)}{n\omega_0 - \Omega} \\ G(u) &= \pi S^2 \rho'(\Omega/n) \end{aligned} \tag{64}$$

Stability boundaries for various spectra are shown Fig.8. When the beam lies in the unstable region, the corresponding instability is called the *longitudinal microwave instability.* Note that Eqs.(63) and (64) are quadratic on the l.h.s.

These are qualitatively different from Eqs.(56) and (59), and are the reason for the qualitative difference between Figs.7 and 8.

The Keil-Schell stability criterion is

$$|(\Delta\omega)_0^2| < 0.68\ n^2 S_{\frac{1}{2}}^2 \tag{65}$$

If $S_{\frac{1}{2}}$ (the spread in revolution frequency ω_0) comes from energy spread, $S_{\frac{1}{2}} = \bar{\omega}_0|\eta|\Delta\delta_{\frac{1}{2}}$, then the condition reads

$$\left|\frac{Z_0^{\parallel}(n\bar{\omega}_0)}{n}\right| < 0.68\ Z_0\frac{|\eta|EC}{2Ne^2}\Delta\delta_{\frac{1}{2}}^2 \tag{66}$$

bunched beam

For a bunched beam, applying the Boussard criterion, Eq.(66) becomes

$$\left|\frac{Z_0^{\parallel}(n\bar{\omega}_0)}{n}\right| < 0.66\ Z_0\frac{|\eta|E}{Ne^2}\Delta\delta_{\frac{1}{2}}^2\Delta z_{\frac{1}{2}} \ = \ 0.66\ Z_0\frac{\omega_s^2 E}{|\eta|c^2Ne^2}\Delta z_{\frac{1}{2}}^3 \tag{67}$$

11 Potential-Well Distortion

The longitudinal wake field distorts the focusing field supplied by the rf, and thus distorts the equilibrium shape of a beam bunch. The mechanism is a static one; no part of the beam bunch is executing collective oscillation. The degree of the distortion increases with the beam intensity. This phenomenon is called the potential well distortion.

Without the wake field, the equilibrium distribution of an electron beam in a storage ring is bi-gaussian in the longitudinal phase space (z, δ), where $\delta = \Delta E/E$. It turns out that the wake field does not disturb the δ part of the

stationary distribution, and only the z-distribution gets distorted, i.e.

$$\psi(z,\delta) = \frac{N}{\sqrt{2\pi}\sigma_\delta} \exp\left(-\frac{\delta^2}{2\sigma_\delta^2}\right) \lambda(z) \tag{68}$$

where $\lambda(z)$ satisfies a transcendental equation, called the *Haissinski equation*,

$$\lambda(z) = \lambda(0) \exp\left[-\frac{z^2}{2\sigma_{z0}^2} + \frac{Ne^2}{\eta\sigma_\delta^2 EC} \int_0^z dz'' \int_{z''}^\infty dz' \, \lambda(z') W_0'(z'' - z')\right] \tag{69}$$

where ω_s is the unperturbed synchrotron frequency, C is the storage ring circumference.

In the limit of zero beam intensity, the solution reduces to the bi-gaussian form, where the unperturbed rms bunch length is $\sigma_{z0} = \eta c \sigma_\delta / \omega_s$. For high beam intensities, $\lambda(z)$ deforms from gaussian. Once $W_0'(z)$ is known and σ_δ specified, the distorted distribution $\lambda(z)$ can be solved numerically using Eq.(69). Fig.9 shows the result of one such attempt for the electron damping ring for the SLAC Linear Collider. The calculated bunch shapes agree well with the measured results shown as open circles.

One feature of Fig.9 is that the distribution leans forward ($z > 0$) as the beam intensity increases. This effect comes from the parasitic loss of the beam bunch, and is a consequence of the real part of the impedance. Since the SLC damping ring is operated above transition, the bunch moves forward so that the parasitic energy loss can be compensated by the rf voltage.

Another feature of Fig.9 is that the bunch length increases as the beam intensity increases. The bunch shape distortion comes mainly from the imaginary part of the impedance. That the bunch *lengthens* is because the imaginary part of the impedance is mostly inductive.

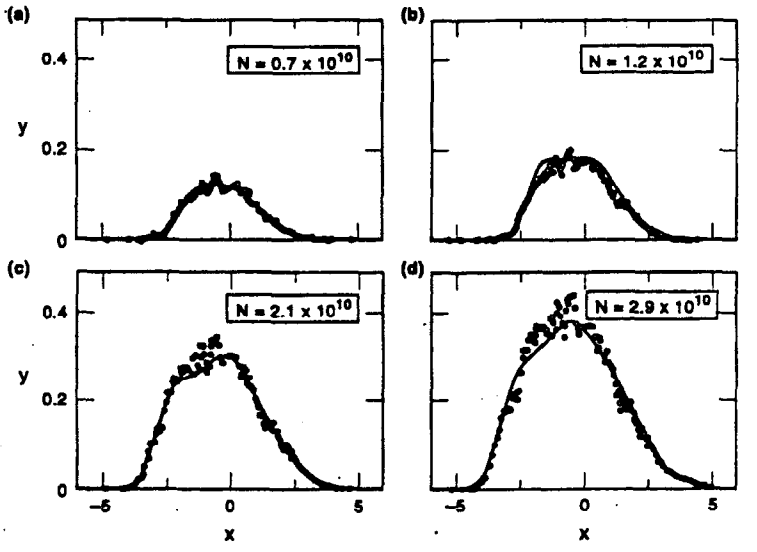

Figure 9: Potential-well distortion of bunch shape for various beam intensities for the SLC damping ring. The horizontal axis is $x = -z/\sigma_{z0}$. The vertical scale is $y = 4\pi N e \lambda(z)/V'_{\rm rf}(0)\sigma_{z0}$.

Find impedance from bunch shape It is possible to extract the impedance $Z_0^{\parallel}(\omega)$ from a detailed measurement of $\lambda(z)$ using a streak camera. Assuming $\lambda(z)$ is determined by potential well distortion alone. Any collective oscillations (e.g. due to microwave instability) are either not present, or averaged out in data averaging with multiple scans.

The procedure to extract $Z_0^{\parallel}(\omega)$ from $\lambda(z)$ is as follows. (i) Calculate the quantity

$$F(z) = \frac{EC\eta\sigma_\delta^2}{Ne^2}\left(\frac{\lambda'(z)}{\lambda(z)} + \frac{z}{\sigma_{z0}^2}\right)$$

(ii) The impedance is then given by

$$Z_0^{\parallel}(\omega) = \frac{1}{c}\frac{\tilde{F}(\omega)}{\tilde{\rho}(\omega)} \tag{70}$$

where $\tilde{F}(\omega) = \int_{-\infty}^{\infty} dz\, e^{-i\omega z/c} F(z)$ and $\tilde{\lambda}(\omega) = \int_{-\infty}^{\infty} dz\, e^{-i\omega z/c}\lambda(z)$.

One disadvantage of this method is that it requires very accurate information on $\lambda(z)$. One advantage is that it allows extraction of the entire impedance, both the real and the imaginary parts, as functions of ω.

12 Bunch Lengthening

Potential well distortion is one mechanism for bunch lengthening, especially when the impedance is primarily inductive (see e.g., Fig.9). This bunch lengthening mechanism does not perturb the energy distribution of the beam, and the distortion in bunch shape is static.

However, there is another mechanism, which involves dynamics and disturbs the beam's energy distribution. This is sometimes called *turbulent bunch lengthening*. Its mechanism nominally (but not always) involves the coupling among the azimuthal modes of beam motion, and becomes important only when the collective mode frequencies shift by amounts comparable to the synchrotron frequency ω_s. The same mechanism was responsible for the transverse mode coupling instability, except now we are in the longitudinal dimension.

The analysis of turbulent bunch lengthening is rather involved. If we ignore the potential-well distortion effect, we end up with solving the eigen-value

problem for the mode frequencies Ω,

$$\det\left(\frac{\Omega}{\omega_s}\,I - M\right) = 0 \tag{71}$$

where I is a unit matrix and M is a matrix with elements

$$M_{\ell\ell'} = \ell\delta_{\ell\ell'} + i\,\frac{Nr_0\eta c^2}{\pi\gamma T_0\omega_s^2\hat{z}^2}\,\ell i^{\ell-\ell'}\int_{-\infty}^{\infty} d\omega\,\frac{Z_0^{\parallel}(\omega)}{\omega}\,J_\ell\left(\frac{\omega\hat{z}}{c}\right)J_{\ell'}\left(\frac{\omega\hat{z}}{c}\right) \tag{72}$$

This result assumes the unperturbed beam has a water-bag distribution in the longitudinal phase space. It also assume a broad-band impedance.

Note that $\Omega = 0$ is always a solution; this is the mode that describes the static potential-well distortion.

As an illustration, we apply the result to the diffractive model, Eq.(13), rewritten as

$$Z_0^{\parallel}(\omega) = R_0\left|\frac{\omega_0}{\omega}\right|^{1/2}[1 + \mathrm{sgn}(\omega)i] \tag{73}$$

where R_0 is a real positive constant. Then,

$$M_{\ell\ell'} = \ell\delta_{\ell\ell'} - \ell\,C_{\ell\ell'}\Upsilon \tag{74}$$

$$C_{\ell\ell'} = \frac{\frac{1}{2}\Gamma\left(\frac{\ell+\ell'-\frac{1}{2}}{2}\right)}{\Gamma\left(\frac{\ell'-\ell+\frac{5}{2}}{2}\right)\Gamma\left(\frac{\ell+\ell'+\frac{5}{2}}{2}\right)\Gamma\left(\frac{\ell-\ell'+\frac{5}{2}}{2}\right)} \times \begin{cases} (-1)^{(\ell-\ell')/2} & \text{if } \ell-\ell' \text{ even} \\ (-1)^{(\ell-\ell'-1)/2} & \text{if } \ell-\ell' \text{ odd} \end{cases}$$

where we have defined a dimensionless parameter

$$\Upsilon = \frac{Ne^2\eta R_0}{E\omega_s^2}\left(\frac{c}{T_0\hat{z}}\right)^{3/2} \tag{75}$$

The eigenvalues Ω/ω_s calculated numerically as functions of Υ for the lowest few modes are shown in Fig.10. At $\Upsilon = 0$, the mode frequencies are simply multiples of ω_s. As Υ increases, the mode frequencies shift. As Υ reaches the

critical value $\Upsilon_{th} \approx 1.45$, the $\ell = 1$ and $\ell = 2$ mode-frequency lines merge, and when $\Upsilon > \Upsilon_{th}$, they become imaginary and the beam is unstable. The parameter Υ_{th} thus defines the instability threshold of the beam.

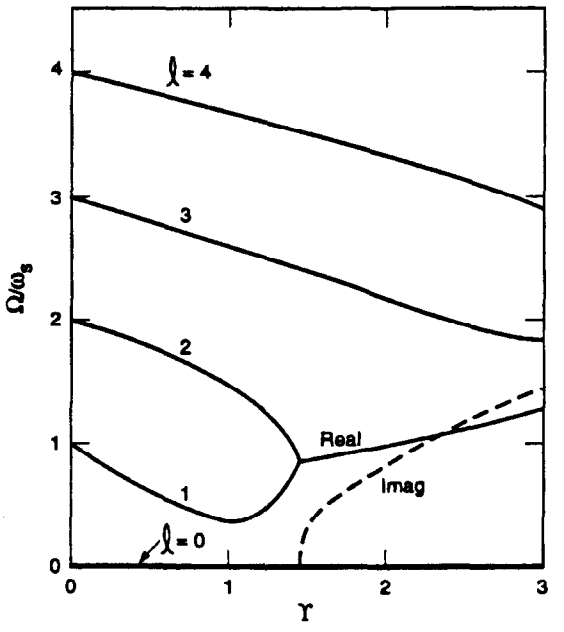

Figure 10: Longitudinal mode frequencies Ω/ω_s versus Υ for a water-bag beam with the diffraction model impedance. The solid curves give the real part of the mode frequencies; the dashed curve gives the imaginary part (magnitude only) of the $\ell = 1$ and $\ell = 2$ mode frequencies above threshold. There is always a static mode with $\Omega = 0$. The spectra for $\ell < 0$ are mirror images with respect to the $\Omega = 0$ line. Potential well distortion has been ignored.

Once a longitudinal mode-coupling instability occurs, one of its consequences is that the bunch lengthens. It lengthens just enough so that Υ stays at the

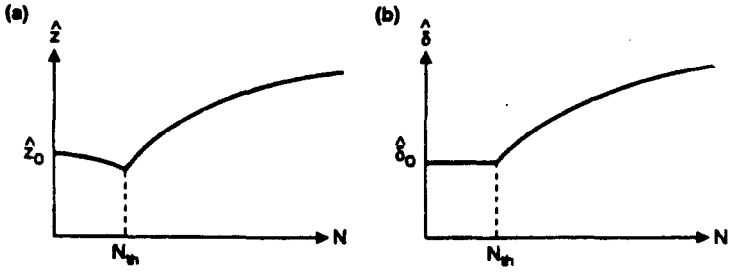

Figure 11: Bunch length $\hat{z}$ and energy spread $\hat{\delta}$ as functions of beam intensity N. Below threshold $N_{\rm th}$, $\hat{z}$ changes due to potential-well distortion, while $\hat{\delta}$ stays constant. Above $N_{\rm th}$, both $\hat{z}$ and $\hat{\delta}$ increase with N. If the impedance is given by the diffractive model, $\hat{z}$ and $\hat{\delta}$ are proportional to $N^{2/3}$ in the region $N > N_{\rm th}$.

instability threshold, i.e.,

$$\hat{z} = \frac{c}{T_0}\left(\frac{Nr_0\eta R_0}{\gamma\omega_s^2\Upsilon_{\rm th}}\right)^{2/3} \tag{76}$$

The behavior of bunch length as a function of beam intensity looks like Fig.11. The curve above the bunch lengthening threshold has $\hat{z} \propto N^{2/3}$. Below the threshold, we have shown a slight potential-well bunch shortening. The change of bunch distribution due to potential-well distortion and that due to mode coupling instability are distinctly different. In the former case, the energy distribution of the beam (we consider an electron beam) is unaffected. In the latter case, the synchrotron oscillation translates the changes in $\hat{z}$ rapidly into proportional changes in $\hat{\delta}$.

Turbulence due to radial mode coupling The above analysis ignores the important potential-well distortion effect. When included, instabilities can result from not only the coupling among azimuthal modes, but also from coupling among radial modes. This leads to a qualitatively different instability behavior. In particular, it might lower the instability threshold, and the mode frequencies do not have to shift as much as $\sim \omega_s$ to reach the threshold. The growth rate, however, tends to be slower in this mechanism because it is quadratic in the beam intensity.

13 Longitudinal Head-Tail Instability

We discussed a head-tail instability and a strong head-tail instability. Both are transverse effects. There is also a head-tail instability in the longitudinal dimension, first observed at CERN-SPS. The "longitudinal head-tail phase" comes from a dependence of the slippage factor η on δ.

Let $\eta = \eta_0 + \eta_1\delta$. Assuming a water-bag model, the longitidinal head-tail instability growth rate for the ℓth mode is found to be, to first order in η_1,

$$\frac{1}{\tau^{(\ell)}} = \frac{4\ell^2\eta_1 Ne^2c}{3\pi\eta_0 EC}\int_{-\infty}^{\infty} d\omega\, \frac{\mathrm{Re}Z_0^{\parallel}(\omega)}{\sigma^2}\left[\sigma J_\ell(\sigma)J_{\ell+1}(\sigma) + (1-\ell)J_\ell^2(\sigma)\right] \qquad (77)$$

where $\sigma = \omega\hat{z}/2c$ and $\ell = 1, 2, 3....$

Physically this instability occurs because of the following. Consider a bunch executing a longitudinal dipole oscillation ($\ell = 1$). Due to $\eta_1 \neq 0$, the bunch length $2\hat{z}$ is a little longer when the bunch has $\delta < 0$ and a little shorter when the bunch has $\delta > 0$ (assuming $\eta_1\eta_0 < 0$). The bunch loses more energy when

it is shorter. This means then that the beam loses more energy when it has $\delta > 0$ and loses less energy when $\delta < 0$. This leads to damping when $\eta_1 \eta_0 < 0$. Instability occurs when $\eta_1 \eta_0 > 0$.

This phenomenon may be important for the *isochronous rings* (considered for synchrotron radiation sources or muon colliders) when $\eta_0 \approx 0$.

14 Further Readings

These notes give a collection of formulas which might come handy in actual calculations. A good fraction of the notes can be found in the *Handbook of Accelerator Physics and Engineering*, ed. A. Chao and M. Tigner, World Scientific (1999), particularly from articles by W. Ng, T. Suzuki, B. Zotter, K. Thompson, K. Yokoya, T. Weiland, R. Gluckstern, S. Kurrenoy, P. Wilson, and A. Piwinski. For discussions emphasizing the physics principles, one may consult *Physics of Collective Beam Instabilities in High Energy Accelerators*, A. Chao, Wiley (1993). For a much more extensive discussion on impedances, one may consult *Impedances and Wakes in High-Energy Particle Accelerators*, B. Zotter and S. Kheifets, World Scientific (1997).